

The infrared conductivity of graphene

N. M. R. Peres,¹ T. Stauber,¹ and A. H. Castro Neto²

¹*Centro de Física e Departamento de Física, Universidade do Minho, P-4710-057, Braga, Portugal and*

²*Department of Physics, Boston University, 590 Commonwealth Avenue, Boston, MA 02215, USA*

(Dated: November 7, 2018)

We study the infrared conductivity of graphene at finite chemical potential and temperature taking into account the effect of phonons and disorder due to charged impurities and unitary scatterers. The screening of the long-range Coulomb potential is treated using the random phase approximation coupled to the coherent potential approximation. The effect of the electron-phonon coupling is studied in second-order perturbation theory. The theory has essentially one free parameter, namely, the number of charge impurities per carbon, n_i^C . We find an anomalous enhancement of the conductivity in a frequency region that is blocked by Pauli exclusion and an impurity broadening of the conductivity threshold. We also find that phonons induce Stokes and anti-Stokes lines that produce an excess conductivity, when compared to the far infrared value of $\sigma_0 = (\pi/2)e^2/h$.

PACS numbers: 81.05.Uw, 73.25.+i, 72.80.-r

Although there has been enormous experimental¹ and theoretical² progress in understanding the physical properties of graphene since its isolation in 2004³, the important issue of graphene transport remains unsettled. More than 20 years ago, E. Fradkin⁴ showed that the D.C. (static) conductivity of graphene, at the charge neutrality point, $\sigma_{D.C.}(\mu = 0) = \sigma(\omega = 0, \mu = 0)$ (ω is the frequency and μ is the chemical potential measured relative to the Dirac point), cannot be described within the standard Boltzmann approach of metals, because the Dirac-like electronic excitations have infinite Compton wavelength (which is cut-off by the size of the sample), violating the assumptions of the validity of Boltzmann transport⁵. Fradkin showed that the proper way to compute the conductivity is through the Kubo formula treating the impurities in a self-consistent way. The Kubo formula predicts a universal, impurity independent, D.C. conductivity: $\sigma_{D.C.,theo.}(\mu = 0) = (4/\pi)e^2/h$. Nevertheless, experiments¹ find that $\sigma_{D.C.,exp.}(\mu = 0) \approx 4e^2/h$ with sample-to-sample variations by a factor of 2, which importantly are in the direction of higher conductivity, i.e., further away from the theoretically predicted value (the so-called mystery of the missing π). This result has been assigned to the macroscopic inhomogeneity and non-local transport in graphene samples¹. Nevertheless, there is still no consensus in the theoretical community on the origin of this effect².

In order to settle the issue of transport and scattering mechanisms in graphene, an aspect of major scientific and technological significance, it is important to study electronic transport away from the static regime. In this regard, the frequency dependent (A.C.) conductivity, $\sigma(\omega, \mu)$ (we use units such that $\hbar = 1$), provides important information on the scattering mechanisms of the charge carriers for frequencies $\omega \lesssim 2\mu$. The basic physical processes involved in the A.C. conductivity are easy to understand. A graphene sample is illuminated with light of frequency ω and vanishing small wavevector that causes creation of particle-hole pairs (pair creation), as shown in Fig. 1. At zero temperature and in the absence of disorder or phonons only particle-hole pairs with energy greater than 2μ are allowed since all the states with energy between $-\mu$ and $+\mu$ are forbidden transitions due to Pauli's exclusion principle. In this case the A.C. conductivity is simply a step

function $\sigma(\omega, \mu) = \sigma_0 \Theta(\omega - 2\mu)$, where $\sigma_0 = (\pi/2)e^2/h$ is the optical conductivity that has been measured recently⁶. The far infrared conductivity is insensitive to phonons, impurities (since these affect only the low energy part of the spectrum) and band structure effects when the frequency of incident light is much larger than 2μ and much smaller than the electronic bandwidth, W (≈ 9 eV)⁷. Nevertheless, as we are going to show, the infrared spectrum is very sensitive to phonons and impurities and the response of the system deviates substantially from the non-interacting clean problem.

Phonons of frequency ω_0 can be either absorbed or emitted by the Dirac electrons. When these phonons are at the center of the Brillouin zone (Γ point) they can be probed by Raman spectroscopy¹, playing an analogous role as light in an A.C. conductivity experiment, that is, creation of particle-hole pairs⁸. Furthermore, impurities play a fundamental role at low energies since it is known that they produce strong broadening of the line-widths⁹. We stress once more, as in the case of D.C. transport, that the impurity broadening has to be calculated self-consistently.

In this paper we compute $\sigma(\omega, \mu)$ taking into account the combined effect of impurities and phonons. We assume that there is a density n_i^C of charge impurities per carbon which might be trapped in the substrate, on top of graphene, or in the interface of graphene and the substrate. We model the screening of charge impurities via the random phase approximation (RPA) together with the coherent potential approximation (CPA), which gives us the self-consistent density of states. We also assume a density n_i of unitary scatterers that exist due to structural disorder (edge defects, cracks, vacancies, etc). The effect of unitary scatterers is only important in producing a finite density of states at the Dirac point and this can be obtained with arbitrarily small values of n_i . We assume throughout the paper that impurities are dilute and the structural disorder is very weak, that is, $1 \gg n_i^C \gg n_i \rightarrow 0$.

We have checked that the effect of in-plane acoustic phonons is negligible and they will be ignored in what follows. We assume that the coupling of graphene to the substrate is strong enough to shift the flexural phonon frequencies away from the infrared regime, allowing us to ignore them for the moment being¹⁰. Hence, we have kept only the optical

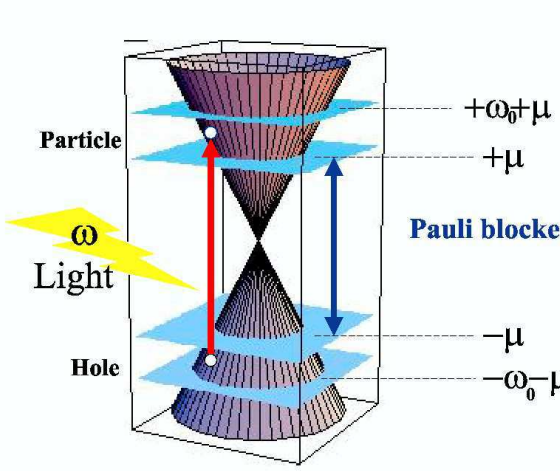


FIG. 1: (color online) A photon of frequency ω creates a particle-hole pair around the Dirac point. The electronic states with energy between $-\mu$ and $+\mu$ are blocked transitions due to the Pauli exclusion principle. In the figure the phonon frequency ω_0 is assumed to be smaller than μ . Light with energy $2 \times (\omega_0 + \mu)$ lead to the generation of an anti-Stokes emission. The Stokes emission with energy $2 \times |\mu - \omega_0|$ lies in the forbidden region.

phonon modes. The phonon frequency, and the value of the electron-phonon coupling is fixed from Raman experiments¹ and therefore they are not fitting parameters here. In fact, we have *only one fitting parameter*, namely, n_i^C .

The Hamiltonian has the form:

$$H = H_0 + H_{\text{ph.}} + H_{\text{e-ph.}} + H_{\text{imp.}}, \quad (1)$$

where

$$H_0 = -t \sum_{\mathbf{R}, \sigma} \sum_{\delta} (a_{\sigma}^{\dagger}(\mathbf{R}) b_{\sigma}(\mathbf{R} + \delta) + \text{h.c.}), \quad (2)$$

is the nearest-neighbor tight-binding kinetic energy where $a_{\sigma}^{\dagger}(\mathbf{R})$ ($b_{\sigma}^{\dagger}(\mathbf{R} + \delta)$) creates an electron on site \mathbf{R} of sub-lattice $A(B)$ with spin σ ($\sigma = \uparrow, \downarrow$), t (≈ 3 eV) is the hopping energy and δ are the nearest-neighbor vectors².

The phonon Hamiltonian has the form^{11,12,13,14,15}:

$$H_{\text{ph.}} = \sum_{\mathbf{R}} \left\{ \frac{\mathbf{P}_A^2(\mathbf{R})}{2M_C} + \frac{\mathbf{P}_B^2(\mathbf{R} + \delta_3)}{2M_C} + \sum_{\delta} \frac{\alpha}{2a^2} [(\mathbf{u}_A(\mathbf{R}) - \mathbf{u}_B(\mathbf{R} + \delta)) \cdot \delta]^2 + \sum_{\delta} \frac{\beta a^2}{2} [\cos(\theta(\mathbf{R}, \delta)) - \cos(\theta_0)]^2 \right\}, \quad (3)$$

where $\mathbf{u}_{A,B}$ are the displacements of the A (B) atoms from equilibrium ($\mathbf{P}_{A,B}$ the momentum operator), M_C ($= 12$ a.u.) is the carbon mass, α (≈ 500 N/m) is the stretching elastic constant, $\theta(\mathbf{R}, \delta) = \theta_{ijk}$ is the angle formed between the $i-j$ bond and the $i-k$ bond ($\theta_0 = 120^\circ$ is the equilibrium angle) and β (≈ 10 N/m) is the in-plane bending elastic constant ($a = 1.42$ Å is the carbon-carbon distance). Although (3) describes both acoustic and optical phonon modes, we focus on the optical modes which can be written as:

$$\mathbf{v}(\mathbf{R}) = (\mathbf{u}_A(\mathbf{R}) - \mathbf{u}_B(\mathbf{R} + \delta_3))/\sqrt{2}, \quad (4)$$

with frequency $\omega_0^2 = 3(\alpha + 9\beta/2)/M_C \approx 0.2$ eV (≈ 1600 cm^{-1})¹².

The electron-phonon Hamiltonian can be written as:

$$H_{\text{e-ph}} = -\frac{1}{a} \frac{\partial t}{\partial a} \frac{1}{\sqrt{N_c}} \sum_{\mathbf{Q}, \mathbf{k}, \sigma, \nu, \delta} \sqrt{\frac{\hbar}{M_C \omega_{\nu}(\mathbf{Q})}} \epsilon_{\nu}(\mathbf{Q}) \cdot \delta \times (B_{-\mathbf{Q}, \nu}^{\dagger} + B_{\mathbf{Q}, \nu}) [e^{i\mathbf{k} \cdot \delta} a_{\sigma}^{\dagger}(\mathbf{k} + \mathbf{Q}) b_{\sigma}(\mathbf{k}) + e^{-i\mathbf{k} \cdot \delta} b_{\sigma}^{\dagger}(\mathbf{k}) a_{\sigma}(\mathbf{k} - \mathbf{Q})], \quad (5)$$

where $\partial t / \partial a \approx 6.4$ eV Å is the electron-phonon coupling, $B_{\mathbf{Q}, \nu}^{\dagger}$ creates a phonon of momentum \mathbf{Q} , polarization ν (polarization vector $\epsilon_{\nu}(\mathbf{Q})$), and frequency $\omega_{\nu}(\mathbf{Q})$ (N_c is the number of unit cells)¹².

The impurity Hamiltonian has the form:

$$H_{\text{imp.}} = \frac{1}{N_c} \sum_{\mathbf{p}, \mathbf{q}, \sigma} V(\mathbf{q}) [a_{\sigma}^{\dagger}(\mathbf{p}) a_{\sigma}(\mathbf{p} + \mathbf{q}) + b_{\sigma}^{\dagger}(\mathbf{p}) b_{\sigma}(\mathbf{p} + \mathbf{q})]. \quad (6)$$

For a screened impurity of bare charge Ze the potential $V(\mathbf{q})$ is given¹⁶ by

$$V(\mathbf{q}) = -\frac{Ze^2}{2\epsilon A_c} \frac{e^{-q d}}{q + \gamma} \quad (7)$$

where $\epsilon = 3.9$ is the SiO_2 relative permittivity, d is the distance of the impurity to the graphene plane, and $\gamma = \rho(\mu) e^2 / (2\epsilon A_c)$ is the RPA screening wavevector² where $\rho(\mu)$ is the self-consistent density of states ($A_c = 3\sqrt{3}a^2/2$ is the area of the unit cell). Unitary scatterers are modeled using a local potential $V(\mathbf{q}) = U$ and taking $U \rightarrow \infty$.

The effect of a dilute concentration of unitary scatterers can be calculated exactly using the T-matrix, leading to a retarded impurity self-energy of the form⁹:

$$\Sigma_R^{\text{unit.}}(\omega) = -\frac{n_i}{\sum_{\mathbf{k}} G_0(\mathbf{k}, \omega + i0^+) / N_c}, \quad (8)$$

where $G_0(\mathbf{k}, \omega)$ is the free electron Green's function associated with Hamiltonian (2). Since $\rho_0(\omega) = -1/\pi \sum_{\mathbf{k}} \Im G_0(\mathbf{k}, \omega)/N_c \propto |\omega|$ is the bare density of states of the clean problem, it is easy to see that (8) leads to a divergence of $\Sigma_R^{\text{unit.}}(\omega \rightarrow 0)$ at the Dirac point which is unphysical. Hence, the problem has to be treated self-consistently by replacing $G_0(\mathbf{k}, \omega)$ by $G^{\text{unit.}}(\mathbf{k}, \omega) = G_0(\mathbf{k}, \omega)/(1 - G_0(\mathbf{k}, \omega)\Sigma_R^{\text{unit.}}(\omega))$ in (8). In this case, one can show that the self-energy becomes finite at the Dirac point¹⁷, as shown in Fig. 2, leading to a finite density of states at zero energy.

The self-energy due to charged impurities is calculated in second order perturbation theory as:

$$\Sigma^C(\mathbf{k}, i\omega_n) = \frac{n_i^C}{N_c} \sum_{\mathbf{p}} |V(\mathbf{k} - \mathbf{p})|^2 G^0(\mathbf{p}, i\omega_n), \quad (9)$$

where a term of the form $n_i^C V(0)$ was absorbed in the definition of the chemical potential. The self-energy (9) is dependent both on the momentum \mathbf{k} and on the frequency. However, we are interested on the effect of the self-energy for momenta close to the Dirac point ($\mathbf{q} = \mathbf{K} = \frac{2\pi}{a}(1/3, \sqrt{3}/9)$). Within this approximation, the imaginary part of the retarded self-energy becomes diagonal and momentum independent, reading ($d \simeq 0$):

$$\Im \Sigma^C(\mathbf{K}, \omega) \simeq -\frac{Z^2 e^4}{4A_c^2 \epsilon_0^2 \epsilon} \frac{n_i^C}{\sqrt{3}t^2} |\omega| \left(\frac{2|\omega|}{3ta} + \gamma \right)^{-2}. \quad (10)$$

Notice that the imaginary part of the self-energy behaves like $|\omega|$ at low frequencies and vanishes as $1/|\omega|$ at large frequencies (see Fig.2).

Hence, the electron Green's function in the presence of impurities is written as: $G^{-1}(\mathbf{k}, \omega) = G_0^{-1}(\mathbf{k}, \omega) - \Sigma^{\text{unit.}}(\omega) - \Sigma^C(\mathbf{K}, \omega)$. Notice that the density of states, $\rho(\omega) = -1/(\pi N_c) \sum_{\mathbf{k}} \Im G(\mathbf{k}, \omega)$, should be computed self-consistently since the screening wavevector γ in (7) and (10) depends on $\rho(\mu)$.

The self-energy due to electron-phonon interaction is also computed at the Dirac point in second order perturbation theory:

$$\Sigma^{\text{opt}}(\mathbf{K}, i\omega_n) = -\frac{9}{2} \left(\frac{\partial t}{\partial a} \right)^2 \frac{1}{M_C \omega_0} \frac{1}{N_c} \sum_{\mathbf{Q}} \times \frac{1}{\beta} \sum_m D^0(\mathbf{Q}, i\nu_m) G(\mathbf{K} - \mathbf{Q}, i\omega_n - i\nu_m) \quad (11)$$

where $D^0(\mathbf{Q}, i\nu_m) = 2\omega_0/((i\nu_m)^2 - [\omega_0]^2)$ is the phonon Green's function. Notice that $G(\mathbf{k}, i\omega_n)$ is the impurity dressed electronic Green's function. Due to the exclusion principle, the imaginary part of the electron-phonon self-energy vanishes when $\mu - \omega_0 < \omega < \mu + \omega_0$, at $T = 0$. At high frequencies the self-energy follows the electronic density of states and is, therefore, linear in ω , as shown in Fig.2.

In the presence of an electromagnetic field the hopping energy changes to:

$$t \rightarrow t e^{ie\mathbf{A}(t) \cdot \boldsymbol{\delta}}. \quad (12)$$

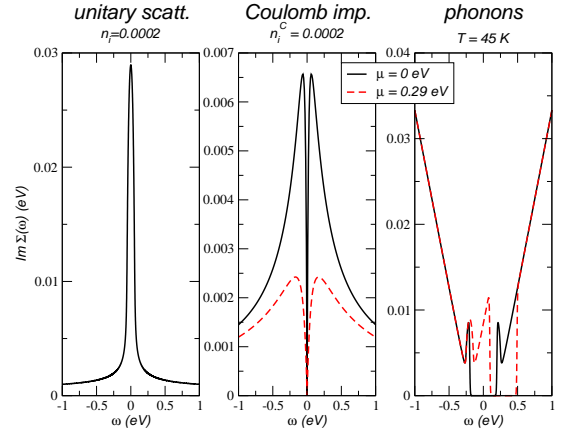


FIG. 2: (color online) Imaginary part of the electronic self-energy due to unitary scatterers, Coulomb impurities, and phonons. The impurity concentration is $n_i = n_i^C = 2 \times 10^{-4}$. We have set $\mu = 0\text{eV}$ (solid line), $\mu = 0.29\text{eV}$ (dashed line) and $T = 45\text{ K}$.

Expanding the exponential up to second order in the vector potential $\mathbf{A}(t)$ and assuming the electric field to be oriented along the x direction, the current operator is obtained from $j_x = -\partial H/\partial A_x(t)$ leading to $j_x = j_x^P + A_x(t)j_x^D$. The Kubo formula for the conductivity is given by:

$$\sigma(\omega) = \frac{1}{A_s} \frac{1}{i(\omega + i0^+)} [\langle j_x^D \rangle + \Lambda_{xx}(\omega + i0^+)], \quad (13)$$

with $A_s = N_c A_c$ the area of the sample and

$$\Lambda_{xx}(i\omega_n) = \int_0^\beta d\tau e^{i\omega_n \tau} \langle T_\tau j_x^P(\tau) j_x^P(0) \rangle, \quad (14)$$

is the current-current correlation function. The finite frequency part of the real part of the conductivity is given by:

$$\Re \sigma(\omega) = \frac{2e^2}{\pi h} \int \frac{d\omega'}{\omega} \Theta(\omega', \omega) [f(\hbar\omega' - \mu) - f(\hbar\omega' + \hbar\omega - \mu)], \quad (15)$$

where $f(x)$ is the Fermi function and $\Theta(\omega', \omega)$ is a dimensionless function that depends on the full self-energy and will be given elsewhere¹⁸. The main features of the conductivity can still be understood from Fig.1. Disorder leads to broadening of the energy levels and a finite density of states at the Dirac point. This implies that the Pauli exclusion is not effective in blocking transitions and hence there is always a finite conductivity even for $\omega < 2\mu$. The conductivity in the “forbidden” region increases with the increase in the number of impurities. The fact that the imaginary part of the electron-phonon self-energy vanishes for electron energies between $\mu - \omega_0$ and $\mu + \omega_0$ indicates that for $2 \times |\mu - \omega_0| < \omega < 2 \times (\omega_0 + \mu)$ the electron-phonon coupling does not produce any effect in the conductivity. For $\mu < \omega_0$, we expect the appearance of an anti-Stokes line at $\omega_{\text{A.S.}} = 2 \times (\omega_0 + \mu)$ and a Stokes line at $\omega_{\text{S.}} = 2 \times (\omega_0 - \mu)$. For $\omega_0 < \mu$ the Stokes line lies inside of the Pauli blocked region and hence it should be suppressed.

In Figure 3 we plot the infrared conductivity of a graphene in units of the far-infrared conductivity $\sigma_0 = \pi e^2/(2h)$. The

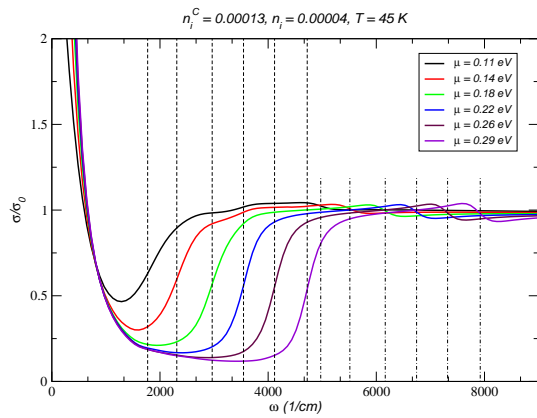


FIG. 3: (color online) Real part of the infrared conductivity including the effect of phonons, unitary scatterers and charged impurities. The parameters are $T = 45$ K, $n_i = 4.0 \times 10^{-5}$, and $n_i^C = 1.3 \times 10^{-4}$. The dashed vertical lines correspond to $\omega = 2\mu$ and the shorter dotted-dashed to $\omega = 2(\omega_0 + \mu)$ for different values of μ .

main feature is that the conductivity is finite in the range $0 < \hbar\omega < 2\mu$ and increases as the gate voltage decreases. We choose the concentration of unitary scatterers states in Fig. 3 to be one order of magnitude smaller than the one of Coulomb scatterers¹⁶, and therefore the conductivity is mainly controlled by phonons and charged impurities. Another feature of the curves in Fig. 3 is the large broadening of the inter-band transition edge at $\hbar\omega = 2\mu$ (indicated by vertical dashed lines). Note that this broadening is not due to temperature but to charged impurities, instead. In fact, the broadening for all values of V_g is larger when the conductivity is controlled by charged impurities. As expected, the coupling to phonons produces a anti-Stokes line centered at $2(\omega_0 + \mu)$. For gate voltages with $\mu < \omega_0$ there appears a Stokes line at $2(\omega_0 - \mu)$. We find, however, that the Stokes line is very sensitive to disorder and is fast suppressed by the inclusion of

charge impurities. The optical phonons thus induce a conductivity larger than σ_0 around these frequencies. This effect is washed out at high temperatures and low frequencies. We also note that for large biases the conductivity in the Pauli-blocked region becomes weakly voltage dependent. All these effects seem to be consistent with the recent infrared measurements of graphene on a SiO_2 substrate¹⁹.

In this paper we have studied the infrared conductivity of graphene at finite chemical potential, generalizing the results of Ref. [9]. The calculation includes both the effect of disorder (unitary scatterers and charged impurities) and the effect of phonons. The effect of acoustic phonons is negligible, since it induces an imaginary part of the electronic self-energy that is much smaller than the imaginary part induced by either impurities or optical phonons. We find that optical phonons and charge impurities produce important modifications in the infrared absorption leading to large conductivities in the Pauli-blocked energy region of $\omega < 2\mu$. The optical phonons also produce a conductivity larger than σ_0 around $2\mu < \omega \simeq 2(\omega_0 \pm \mu)$ due to Stokes and anti-Stokes processes. It is interesting to note that for frequencies away from the Dirac point the imaginary part of the self-energy due to optical phonons is linear in frequency, a behavior similar to that due to electron-electron interactions in graphene². The most important approximation in our calculations is associated with the fact that we have neglected completely flexural modes since we assume that they are pinned by the substrate and hence have very high excitation energy, that is, away from the infrared regime. We stress that the only free parameter in the calculation is the density of charge impurities, n_i^C that can change from sample to sample.

We thank D. N. Basov, A. K. Geim, F. Guinea, P. Kim, and Z. Q. Li for many illuminating discussions. We thank D. N. Basov, and Z. Q. Li for showing their data prior to publication. N.M.R.P. and T.S. were supported by the ESF Science Program INSTANS 2005-2010, and by FCT under the grant PTDC/FIS/64404/2006.

¹ For a review on the experimental issues, see A. K. Geim and K. S. Novoselov, *Nature Materials* **6**, 183 (2007), and references therein.

² For a review on the theoretical issues, see A. H. Castro Neto, F. Guinea, N. M. R. Peres, K. S. Novoselov, and A. K. Geim, *Rev. Mod. Phys.* [in press], arXiv:0709.1163, and references therein.

³ K. S. Novoselov, A. K. Geim, S. V. Morozov, D. Jiang, Y. Zhang, S. V. Dubonos, I. V. Grigorieva, and A. A. Firsov, *Science* **306**, 666 (2004).

⁴ E. Fradkin, *Phys. Rev. B* **33**, 3263 (1986).

⁵ J. M. Ziman, *Electrons and Phonons* (Oxford University Press, London, 2001).

⁶ A. K. Geim, private communication.

⁷ T. Stauber, N. M. R. Peres, and A. K. Geim, arXiv:0803.1802.

⁸ A. H. Castro Neto, *Nature Materials* **6**, 176 (2007).

⁹ N. M. R. Peres, F. Guinea, and A. H. Castro Neto, *Phys. Rev. B* **73**, 125411 (2006).

¹⁰ The effect of flexural modes can be analyzed in a similar way but it will introduce new free parameters that have to be adjusted experimentally. Here, we simplify by considering a single adjustable parameter.

¹¹ L. M. Woods and G. D. Mahan, *Phys. Rev. B* **61**, 10651 (2000).

¹² Hidekatsu Suzuura and Tsuneya Ando, *Phys. Rev. B* **65**, 235412 (2002).

¹³ Tsuneya Ando, *J. Phys. Soc. Jpn.* **75**, 124701 (2006).

¹⁴ Kohta Ishikawa and Tsuneya Ando, *J. Phys. Soc. Jpn.* **75**, 84713 (2006).

¹⁵ A. H. Castro Neto and F. Guinea, *Phys. Rev. B* **75**, 45404 (2007).

¹⁶ T. Stauber, N. M. R. Peres, and F. Guinea, *Phys. Rev. B* **76**, 205423 (2007).

¹⁷ P. A. Lee, *Phys. Rev. Lett.* **71**, 1887 (1993).

¹⁸ N. M. R. Peres, T. Stauber, and A. H. Castro Neto, unpublished.

¹⁹ Z. Q. Li *et al.*, unpublished.